Paper No.
06436

CORROSION
NACExpo 2006
61ST ANNUAL CONFERENCE & EXPOSITION

# HYDROGEN FLUX AND HIGH TEMPERATURE ACID CORROSION

Frank W.H. Dean
Ion Science Ltd
The Way, Fowlmere,
Royston, SG8 7UJ, UK

Stephen W. Powell
Ion Science Ltd
The Way, Fowlmere,
Royston, SG8 7UJ, UK

## ABSTRACT

There has been recent interest in the use of hydrogen flux monitoring at high temperatures to evaluate 'naphthenic acid' and sulfidic corrosion in high temperature process streams associated with crude distillation units. In this report, we present flux and corrosion data obtained from samples drawn from a refinery process stream.

## INTRODUCTION

For the purposes of this paper high temperature acid corrosion is defined as corrosion of steel due to contact with a proton bearing liquid at above 100 $^{o}$C. Of particular interest is naphthenic acid corrosion and sulfidic corrosion of steel, encountered in refinery service equipment processing crude fractions at temperatures between approximately 200 and 400 $^{o}$C. Atmospheric and vacuum distillation, light and heavy vacuum oil (LVGO, HVGO), and coker units are affected.

Naphthenic acid is a generic term for a range of aliphatic cyclic mono- and poly-carboxylic acids found in crude oil. It is known that the total acid number (TAN) of a crude or crude derivative, expressing milligrams of KOH required to neutralise 1 g of sample, does not provide a sure indicator of corrosivity since the distribution of naphthenic acids within crude blends varies widely, and the corrosivity of individual acids vary, primarily, with molecular weight [1], probably in so far as that affects reaction kinetics, the solubility of the iron salt formed, and the ability of the acid to solubilise iron sulfide formed on the iron surface formed as a consequence of sulfidic corrosion[1-4];

$$Fe + H_2S \rightarrow FeS + H_2 \text{ or } 2H \text{ [Fe surface]} \quad (1)$$

$$FeS + 2RCOOH \text{ (naphthenic acid)} \rightarrow Fe(OOCR)_2 + H_2S \quad (2)$$

Naphthenic acid bearing fluids are of low conductivity[4], and it is considered that naphthenic acid corrosion is predominantly chemical in nature. Schematically,

$$Fe + RCOOH \rightarrow Fe\text{-}OOCR\ [Fe\ surface] + H\ [Fe\ surface] \quad (3)$$
$$Fe\text{-}OOCR + RCOOH \rightarrow Fe(OOCR)_2\ H\ [Fe\ surface] \quad (4)$$

Electrochemical corrosion is conceivable over very small electrolytic pathways within micro corrosion cells:

$$RCOOH + e^- \rightarrow RCOO^- + H\ [Fe\ surface] \quad (5)$$
$$Fe + 2RCOO^- \rightarrow Fe(OOCR)_2\ 2e^- \quad (6)$$

In either case atomic hydrogen is liable to be formed on the iron surface. There from, it may diffuse into (and out of) the steel as in (7) or form molecular hydrogen, desorbed into the process stream, by a variety of conceivable reactions such as (8-10):

$$H\ [Fe\ surface] \leftrightarrow H\ [in\ Fe] \quad (7)$$
$$2H\ [Fe\ surface] \rightarrow H_2\ [Fe\ surface,\ desorbed] \quad (8)$$
$$Fe + H\ [Fe\ surface] + RCOOH \rightarrow H_2\ [Fe\ surface,\ desorbed] + Fe\text{-}OOCR\ [Fe\ surface] \quad (9)$$
$$H\ [Fe\ surface] + RCOOH + e^- \rightarrow H_2\ [Fe\ surface,\ desorbed] + RCOO^- \quad (10)$$

A proportion of hydrogen entering steel *via* (7) could conceivably permeate through the entire steel wall, to arrive at, form molecular hydrogen at, and desorb from, the exit face, measurable as a hydrogen flux. Such hydrogen flux measurements in the field have been reported, which indicate test site position dependence [5], and co-trending of flux measurements at different sites during process stream variation over time[6]. Corrosion induced hydrogen permeation has also been demonstrated to occur in the case of mineral acid (Na/K hydrogen phosphate eutectic) at 150-310 $^oC$ [7]. The objective of this work was to investigate the hydrogen flux induced as a function of corrosivity of some representative crude samples and temperature, to qualify the emergent use of hydrogen flux measurement as an active high temperature acid corrosion indicator in the field.

## EXPERIMENTAL METHOD

Crucibles were manufactured by welding one end of 110 mm inner diameter, 200 mm length of 9 Cr steel tube, to a 150 mm square base plate, of 6.4 mm thickness AISA 1018 carbon steel. A crucible base plate was placed centrally on a 'hydrogen collection' probe plate connected to a hydrogen flux analyser[1]. The capillary leading from the probe was inserted through two inches of insulation and a hole in a bench supporting the entire apparatus as shown in Figure 1a and b.

A flexible ceramic heat mat was affixed with wire around the crucible, and overlaid with 50 mm of rock wool insulation. A lid of stainless steel was constructed for the crucible, into which was centrally affixed a 10 mm inner diameter Kovar tube connected via glass joints to a Friedrich condenser and gas bubbler. Through another drilled and tapped hole in the lid was affixed a capillary, whose free end provided admittance of 100 mL/min 99.999% argon[2] to the base of the crucible. Through a further hole was inserted a K type thermocouple, such that when the lid was closed, the thermocouple would be located about 1 cm from the base of the crucible.

[1] Hydrosteel AT-S probe and 6000 analyser, Ion Science Ltd, UK
[2] BOC

Before each trial, the crucible lid was removed, liquid residue from the previous trial extracted by syringe, and all internal crucible surfaces scrubbed with several aliquots of diisopropyl ether. The base of the crucible was ground to a P1000 grit finish, and wiped clean with ether. A corrosion coupon of 10.5 cm length, cut from the same carbon steel as the crucible base was ground with SiC paper to P1000 finish, weighed, and placed in the bottom of the crucible as illustrated in Figure 1b. The HVGO sample, a grease at room temperature, was liquefied in a microwave oven, then agitated. For each trial, 300 mL of a process sample was poured into to the crucible, sufficient to fully cover the coupon. The lid was closed, a seal forming between it and the crucible by virtue of high temperature vacuum grease[3] applied to the lid perimeter.

The argon flow was increased to thoroughly purge the system of air for 20 minutes before commencement of each trial. Throughout each trial, argon flow was observed through the bubbler. In the occasional early trial, rapid condensation in the refluxer occasionally led to air suck-back into the system, which blackened sample fluid. Results from such trials were considered unreliable and are not presented.

The heat mats were powered by two mains transformers delivering a total of 2.8 kW power. A PID temperature controller[4] regulated power supply to the crucible on the basis of temperature indicated by a K type thermocouple abutting the inner surface of the heat mat. Temperature was further indicated from the crucible thermocouple. This temperature was frequently recorded, and is presented together with hydrogen flux data below. Experiments were conducted under a prescribed elevated temperature regime for at least 5 hr. After the sample fluid had cooled to less than 100 deg C, the lid was breached and coupon removed and reweighed, after cleaning in methanol and 'Super Clarkes' solution.

The flux measurement apparatus is described in detail elsewhere.[(8-10)] Briefly, during trials, a pump in the analyser caused ambient air to be drawn from across the entire surface of the base plate opposing the corroding surface, by means of a spiral groove on the probe underside shown in Figure 1c, and thence through the probe's central capillary and leading to a hydrogen analyser. The analyser recorded the hydrogen flux $J$ (pL.cm$^{-2}$.s$^{-1}$), given by $1000F.c/\mathbf{A}$, where $c$ (ppm v/v) is the increase in hydrogen concentration in air registered by the analyser, $F$ (mbar.L.s$^{-1}$) is the air flow rate, and **A** is the probe's effective hydrogen capture cross section. Output analyser readings were linearly adjusted for a value of **A** set equal to the base plate's interior surface area; it was assumed that the diameter of the exit flux capture surface sufficiently exceeded the corroding surface diameter, relative to the plate thickness to substantially capture all hydrogen flux issuing therefrom[5].

Field samples were designated 'HVGO', 'LVGO' and 'red' (crude bottom). Only one data set from a successful trial with synthetic corrosion liquor is presented, namely 'CPCA'. This comprised 0.25 M cyclopentane carboxylic acid[6] in heavy mineral oil.[7]. Evaluations of further synthetic solutions, using heavier naphthenic acids', are underway.

---

[3] Apiezon
[4] Eurotherm 2132
[5] Hydrogen permeation is substantially determined by Fick's Law of diffusion, that is, at any point in the steel the hydrogen flux is proportional to the diffusible hydrogen concentration gradient, and directed normal to the plane of equal hydrogen concentration at that point. Thus hydrogen entry at the perimeter of the hydrogen entry surface is somewhat increased, and exits over an extended surface. A further complication is enhanced diffusion parallel to a plate, derived from grains being elongated in that direction during milling, although this will be of less consequence at elevated temperatures than at ambient temperatures. These positive and negative edge effects would have been avoided by using a smaller probe, which would however introduce greater inaccuracy according to the flux measurement principle.
[6] Aldrich
[7] Fluka

## RESULTS

Flux transients and temperature profiles themselves are presented in Figures 2-5. In Figure 2, the initial 'flux' peaks were attributed to bake out of hydrogen from the sampled steel, and ambient hydrogen generated by burn off of insulation binder. The latter was evident from routine sampling of ambient gas under insulation, prior to each temperature step increase, which confirmed that subsequent hydrogen backgrounds were negligible. It is worth noting that similar burn off of binder is likely in field applications following the installation of the fixed flux probes identical to that used in this work under (new) insulation. Thus field hydrogen flux measurements are possibly only reliable a day or two after fixed probe installation and pipe re-cladding.

Figures 2-4 also indicate field operating temperatures. Temperature excursions below and above these temperatures were carried out as the objective of the work was to correlate flux and corrosion over varied temperatures. The maximum temperature was constrained by sample reflux. In the case of LVGO sample, Figure 2, condensate was observed at 280 $^{o}$C and reflux at 390 $^{o}$C. For the red crude sample, Figure 4, condensate appeared at about 300 $^{o}$C, and reflux at 385 $^{o}$C. However, in both red crude trials, the maximum fluid temperature peaked at 400 $^{o}$C, presumably due to elimination of non-condensates after hydrocarbon cracking.

Table 1 summarizes data obtained in trials conducted hitherto. The final column was obtained by summing over time the hydrogen activity obtained from flux-temperature data for an entire trial, and is believed to deliver the best estimate of corrosivity (see *Discussion*). Coupon wall losses were calculated from their (total) surface area and weight loss under trial. 0.047 μm was subtracted from all data in view of unavoidable oxidation of coupons in air which in blank tests were found to cause a consistent equivalent weight loss.

## DISCUSSION

Figures 2-4 indicate that flux decayed, typically, by some 40% per hour, at each incremental step temperature. The decay was some ten times slower in the case of 0.25 molar CPCA in mineral oil, Figure 5. Field samples were expected to contain higher molecular weight naphthenic acids and sulfur species, whose corrosion products are understood to passivate steel more effectively than CPCA. Significantly, they also included a 'residual' phosphate based high temperature inhibitor. This inhibitor activated at 180 $^{o}$C. In RED crude Trial 2, Figure 4, the fluid was maintained at 210 $^{o}$C for an extended time, before subjecting it to the same temperature step routine as Trial 1. Flux at each temperature step were reduced approximately 10-fold, indicating that the inhibitor was probably primarily responsible for flux decay, although high molecular weight naphthenic acid corrosion products can "block" the surface, and should not be discounted.

It is also somewhat reassuring that the flux decay rate we observed with CPCA was similar to the rate of *corrosion* rate decay found by Slavcheva *et al.*, also on a carbon steel, also at 0.25 M in mineral oil, albeit at a higher temperature (275 vs 212 $^{o}$C). However, in comparing fluxes with the corrosion rate at different temperatures we should note that hydrogen solubility and diffusivity through steel increases with temperature. Thus we might anticipate an increase in flux with temperature, even if the corrosion rate remains unchanged.

Slavcheca *et al.* present an Arrhenius plot (log corrosion rate vs 1/T) for corrosion by cyclohexane carboxylic acid (CHCA, a 7-carbon naphthenic acid, vs 6-carbon CPCA) in order to identify the

activation energy for corrosion, and thus its temperature dependence. Figure 6 shows an Arrhenius plot of log(peak flux) vs 1/T. The data is striking. With the exception of data at increasing stepped temperatures after the extended dwell at 210 $^{o}$C in RED crude trial 2, and at 290 $^{o}$C in HVGO trial 2, data sets for the three field samples are clearly distinguished. With the same exceptions, trial data is inclined at a gradient equal to, or more negative than, that for log(hydrogen Permeability, P) data, also plotted.

Now the hydrogen activity at a corroding face $a_0$, in units of bar$^{1/2}$ (molecular hydrogen), is related to through wall flux and permeability by:

$$a_0 = \mathbf{J^*w}/P \qquad (11)$$

where J (pL.cm$^{-2}$.s$^{-1}$) is the flux, **w** (cm) is the wall thickness, and P (pL.cm$^{-1}$.s$^{-1}$.bar$^{-1/2}$) is the permeability. P varies with temperature as

$$P = P_0 \exp ( -E_a / RT) \qquad (12)$$

where $P_0$ is a constant (equal to the permeability at infinite temperature) and $E_a$ the is the activation energy for permeation. Therefore a log(flux) data set for a particular trial running parallel to the permeability plot in Figure 6 indicates that the hydrogen activity $a_0$ was independent of temperature. A plot of more negative uniform gradient indicates log $a_0$ increasing with 1/T linearly, just as is expected and demonstrated by Slavcheva *et al.*[1] in their Arrhenius plot of CHCA corrosion data. Therefore we anticipate some linear correlation between corrosion rate ***r*** (mm/yr) and activity:

$$\boldsymbol{r} = C.\, a_0 \qquad (13)$$

where $C$ is a constant. Now since $\boldsymbol{r}$ = dw/(A.ρ.dt), where A and ρ are constant, namely the surface area and density of the coupon respectively, it follows that A.ρ.$\int \boldsymbol{r}$.dt, the coupon weight loss sustained over the time of a trial, should be equated with $C.\int a_0.$dt; the sum of activity during that time. The sum $\int a_0.$dt was calculated from equations (11) and (12), using Grabke and Riecke's permeability data for carbon steel[11], from flux and temperature data for each trial shown in Figures 2-5. Data is presented in the final columns of Table 1 and illustrated in Figure 7. The correlation is fair for all but the LVGO data, especially when it is considered that the data spans very disparate samples and trial temperature regimes. The LVGO data is possibly inaccurate due to both low prevailing flux and coupon weight loss. Correspondingly, we have fixed our correlation on the data point provided by the CPCA trial, simply because the flux and weight loss data from which it is derived is largest and thus least prone to inaccuracy.

The linear relationship between corrosion rate and activity at elevated temperatures, equation (13) and Figure 7, was somewhat unexpected. Dean[12] reported an inverse relation between flux and thickness **w** for carbon steel at 19 $^{o}$C, according to equation (11), for steel of thickness greater than ~0.5 cm. For thinner steel at this temperature, the permeation of hydrogen is no longer under exclusively bulk permeation control. Hydrogen permeability through carbon steel is some 110 times lower at 300 $^{o}$C than at 19 $^{o}$C, so we had anticipated flux through the 6.4 mm steel at elevated temperatures to be determined more by hydrogen entry kinetics, and to be less permeation dependent. Substantially, it appears not to be. A flux thickness relationship at elevated temperatures should be investigated.

Using the linear correlation constant, $C$, derived from the above approach, flux and temperature data at any time can be converted to corrosion rates using equations (11) to (13). Maximum, and 'inhibitor

stabilised' corrosion rates for the three samples at operating temperatures quoted is given in Table 2. Corrosion from the LVGO sample is markedly lower, possibly in part due to its low TAN.

Inhibitor stabilisation, and or, corrosion blocking by high molecular weight corrosion product was incomplete in the time scale of the trials, and field corrosion rates are likely to be substantially lower than those cited due to both the very prolonged exposure time of service steel, and higher prevailing inhibitor concentrations in the process stream anywhere upstream of the points of sample withdrawal.

We also consider that the very much steeper temperature dependency of CHCA corrosion indicated by Figure 8 is more usual of high temperature acid corrosion, again, reflecting the major role of inhibitor in passivating field sample corrosion.

## CONCLUSIONS

Allowing for the presence of inhibitor in three field process stream samples, log(flux) vs 1/T plots indicated behaviour consistent with a linear correlation between corrosion rate and hydrogen entry face activity. This was confirmed from approximately linear correlation between the activity-hours of flux simultaneously measured through wall of carbon steel, and weight loss sustained by a coupon of same material, sustaining the same corrosion regime.

Corrosivity of HVGO and red crude samples were substantially higher than LVGO. Corrosion rates from all three would be expected to be <0.1 mm/yr within a few hours exposure of freshly revealed steel at their respective operating temperatures, due to residual inhibitor present in the samples.

It is considered that flux data can be used to rapidly determine the corrosivity of crude distillate fractions at specified temperatures to at least 400 $^{o}$C, and the real time impact on corrosivity of co-present residual inhibitor and inhibitive scale. However, further data is needed to support the correlation shown in Figure 7. Firstly, it would be an advantage to test field samples without traces of inhibitor. In due course, other steels used in high temperature service, particularly 5 and 9 Cr, need to be evaluated, as should other steel thicknesses and the effect of sheer velocity, to confirm correlation developed herein.

**TABLE 1**
**SUMMARY OF TRIALS**

| Liquor | TAN | S | Trial no | Maximum trial temperature | Coupon weight loss | Hydrogen activity-hours |
|---|---|---|---|---|---|---|
| | mg KOH / g | ppt | | Deg C | mg | $bar^{1/2}$.hr |
| LVGO | 1.60 | 0.29 | 1 | 294 | 3.9 | 0.146 |
| | | | 2 | 388 | 1.7 | 0.033 |
| HVGO | 2.20 | 0.33 | 1 | 292 | - | 0.361 |
| | | | 2 | 396 | 4.0 | 0.305 |
| RED | 2.29 | 0.32 | 1 | 401 | 5.7 | 0.534 |
| | | | 2 | 388 | 4.3 | 0.263 |
| CPCA | 18.00 | 0.00 | 1 | 212 | 106 | 9.907 |

**TABLE 2**
**Carbon steel corrosion rates at operating temperatures inferred from activity - corrosion correlation developed in the text. The italicized value is interpolated.**

| Sample | TAN | S | Maximum operating T | Max. corrosion rate | Max. 'inhibitor stabilised' corr. rate |
|---|---|---|---|---|---|
| | mg KOH / g | ppt | $^{o}$C | mm/yr | mm/yr |
| LVGO | 1.60 | 0.29 | 266 | 0.03 | 0.03 |
| HVGO | 2.20 | 0.33 | 360 | *0.4* | 0.1 |
| RED | 2.29 | 0.32 | 350 | 0.53 | 0.045 |

## FIGURES

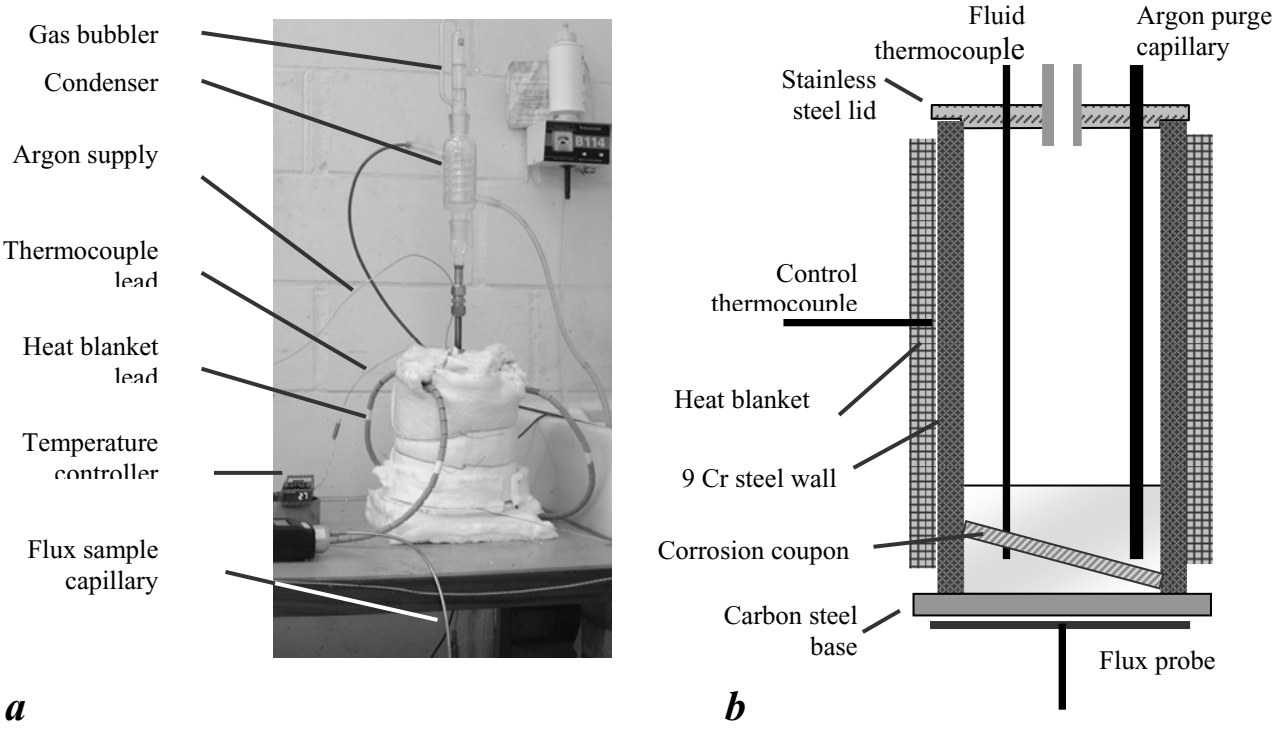


***a*** ***b***

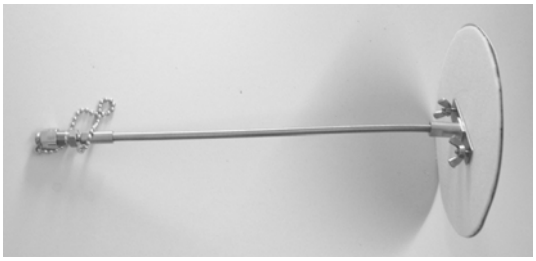

***c***

**FIGURE 1, *a*: photograph of distillation apparatus. *b*: schematic of cross section of crucible under trial, indicating location of key components.**
***c* : hydrogen flux probe**

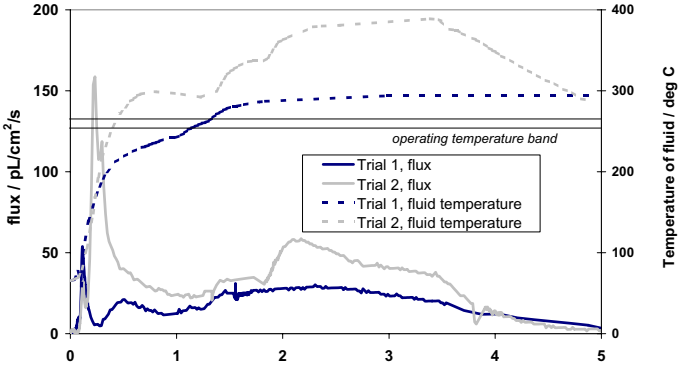


**FIGURE 2 - LVGO flux transients from two trials, subject to indicated temperature excursions.**

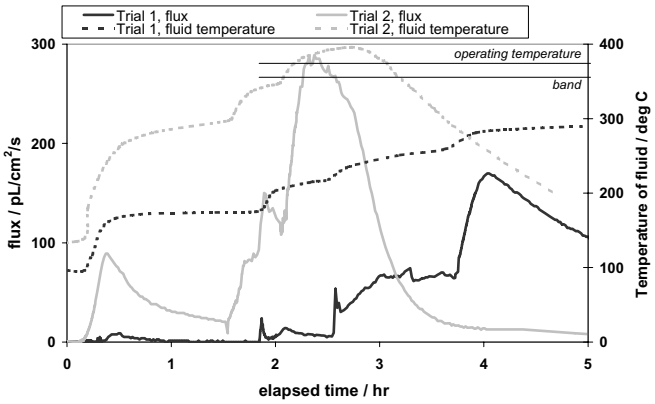


**FIGURE 3 - HVGO flux transients from two trials, subject to identified fluid temperature excursions.**

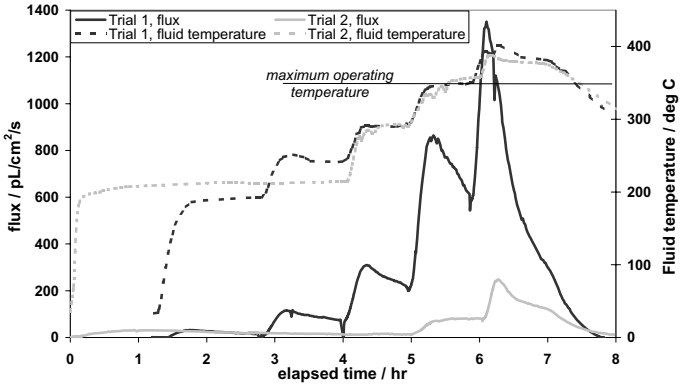


**FIGURE 4 - red crude flux transients, subject to identified fluid temperature excursions**

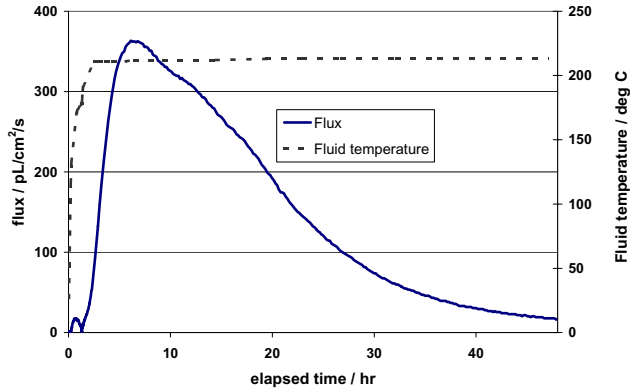


**FIGURE 5 - CPCA in mineral oil, subject to identified fluid temperature excursion. Note extended time scale as compared with Figures 2-4.**

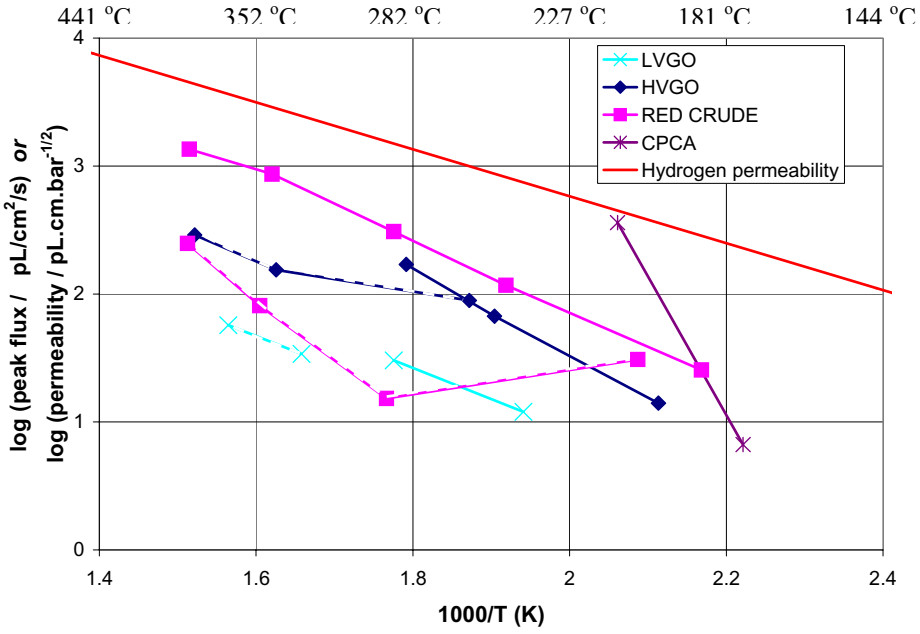


**FIGURE 6 - An Arrhenius-type plot of log(peak flux) *vs* reciprocal temperature. Dashed lines refer to Trial 2 data. The plot for carbon steel permeability is also shown for comparison.**

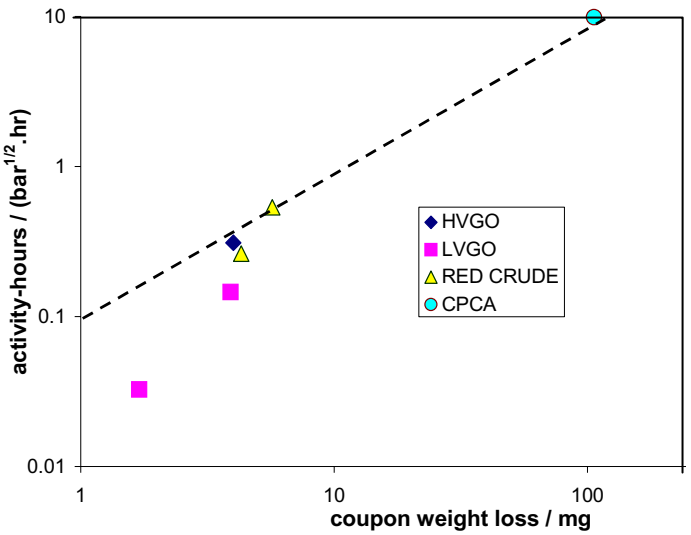


**FIGURE 7 - correlation of corrosion weight loss with hydrogen activity derived from summing over the time of flux profiles shown in Figures 2-4.**

## ACKNOWLEDGEMENTS

The authors would like to thank Chevon Corporation for provision and analysis of field samples evaluated in this work.

## REFERENCES

1 E.Slavcheva, B.Shone, A.Turnball, *Corrosion 1998*, Paper 579, NACE Intl. Conference.

2 H.Craig, Proc. Conf, *Corrosion 1996*, Denver, CO, Paper 603, (Houston, TX: NACE, 1996).

3 R.D.Kane, M.S.Cayard, *Corrosion 2002*, San Diego, CA, Paper 02555 (Houston, TX: NACE, 1996).

4 E.Slavcheva, B.Shone, A.Turnball, *British Corrosion J.*, **34(2)** (1999), 125.

5 F.W.H.Dean, Corrosion 2002, NACE, paper 02344, (Houston, TX: NACE, 1996).

6 A.M.Etheridge, E.B.McDonald, D.Go Serate, F.W.H.Dean, *Corrosion 2004,* Paper 04478

7 F.W.H.Dean, D.J.Fray, T.M.Smeeton, *J.Materials Sci. and Technology*, **18** (2002), 851.

8 F.W.H.Dean, D.J.Fray, *J.Materials Science and Technology*, **16** (2000), 41-49.

9 F.W.H.Dean, A.E.Ling, US Patent 6,637,253

10 F.W.H.Dean, A.E.Ling, European Patent Appl. 00311501.1

11 H.J.Grabke, E.Riecke, *Mater. Tehnol.*, **34(6)** (2000), 331-341.

12 F.W.H.Dean, *J.Materials Science and Technology*, **21(3)** (2005), 347-351.